Journal of Alloys and Compounds 509 (2011) 3924–3930

Contents lists available at ScienceDirect

Journal of Alloys and Compounds

journal homepage: www.elsevier.com/locate/jallcom

Chemical trends of the band gaps of idealized crystal of semiconducting silicon clathrates, $M_8Si_{38}A_8$ (M = Na, K, Rb, Cs; A = Ga, Al, In), predicted by first-principle pseudopotential calculations

Yoji Imai [a,*], Motoharu Imai [b]

[a] National Institute of Advanced Industrial Science and Technology (AIST), AIST Tsukuba Central 5, Higashi 1-1, Tsukuba, Ibaraki 305-8565, Japan
[b] National Institute for Materials Science (NIMS), Sengen 1-2-1, Tsukuba, Ibaraki 305-0047, Japan

ARTICLE INFO

Article history:
Received 29 November 2010
Received in revised form
22 December 2010
Accepted 22 December 2010
Available online 30 December 2010

Keywords:
Silicon-clathrate
Semiconductor
$K_8Si_{38}Ga_8$
Electronic structure

ABSTRACT

We have calculated the band structures of Si clathrate, $M_8Si_{38}Ga_8$ (M = Na, K, Rb, and Cs), using the density-functional theory under the generalized gradient corrected local density approximation, where M is the encapsulated guest alkali atom. They are found to be indirect semiconductors with the calculated gaps (E_g) from 0.45 to 0.89 eV, which should be compared to the calculated gap of 0.65 eV of crystalline Si with the diamond structure. The gaps become wider with the promotion to the heavier guest alkali atoms and the reasons of gap widening are discussed using the calculated dependence of E_g on the cell-volume of guest-free silicon clathrate (Si_{46}). Effect of the substitutional elements in the clathrate framework (Al and In in place of Ga) was also discussed.

1. Introduction

Since Kasper et al. discovered that Si and Ge can form clathrate frameworks with guest metal atoms encapsulated into the 'cages' of the structure [1], a wide variety of the 14th group clathrates have been synthesized by incorporation of impurity atoms. As for theoretical investigation of clathrates, Adams et al. found that the guest-free, elemental, Type-I silicon clathrate (Si_{46}) is a semiconductor[1] with a wider band gap than Si with the diamond structure (di-Si) in 1994 [2]. This work evoked the interest in this material as electronic materials. In 1995, Kawaji et al. found the superconductivity of $(Na, Ba)_xSi_{46}$ [4] and, in 1998, Nolas et al. proposed that Ge Type-I clathrates are attractive as thermoelectric materials since the rattling motion of guest atoms will reduce the thermal conductivity [5].

Since then, most of the experimental works have been focused on (1) synthesizing Ge-clathrate as thermoelectric materials or (2) superconductivity of Ba_xSi_{46}-like clathrates. We suppose that Si-based semiconducting materials seem to be worth while to study for thermoelectric and other energy-conversion materials such as solar cells from the viewpoint of elemental abundance, environmental protection, and the economy. However, researches on semiconducting Si clathrates have been relatively rare.

We recently synthesized $K_8Ga_8Si_{38}$ and confirmed that this is a semiconductor, though estimated band gap value, E_g, from resistivity and optical absorption is much narrower than the value of theoretical prediction [6].

The discrepancy of observed E_g from theoretical prediction may be caused by several reasons such as (1) the random positioning of the atoms, which cannot be modeled in normal band calculations, (2) vacancies which introduce dangling bond states, (3) effect of higher temperature than 0 K, and (4) deviation from ideal stoichiometry [7].

However, we consider that it is significant to know how the encapsulated guest alkali atoms, M (=Na, K, Rb, and Cs), and the substitutional 13th group elements into the clathrate framework, A (=Ga, Al, In), will influence the E_g value of Si clathrate for further understanding. Therefore, we performed systematic calculations of the Si clathrate phases, $M_8Si_{38}A_8$, and tried to clarify the effect of M and A on the band gaps using first-principle calculations, though some of them are as yet unsynthesized.

* Corresponding author. Tel.: +81 29 861 4440; fax: +81 29 861 4440.
E-mail address: imai-y@aist.go.jp (Y. Imai).

[1] Adams et al. claimed that Si_{46} is an indirect semiconductor with the valence band maximum located along Γ to X and the conduction band minimum located at Γ [2]. Later, Connétable et al. claimed that Si_{46} is a direct semiconductor with the conduction band minimum also located along Γ to X [3]. Our result was close to the latter, as stated later, where difference in the energy at Γ and conduction band minimum was as small as 34 meV.

0925-8388/$ – see front matter © 2010 Elsevier B.V. All rights reserved.
doi:10.1016/j.jallcom.2010.12.171

2. Methods

2.1. Compounds considered

At first, we briefly describe the structure of Type-I clathrate for ease of understanding. The Type-I 14th group elements clathrates are characterized by fullerene-like polyhedra; dodecahedra (T_{20}) and tetrakaidecahedra (T_{24}). Here, T is an atom of the 14th group, tetrel. There are two T_{20} and six T_{24} units in each unit cell of the simple cubic structure, belonging to the space group *Pm*-3*m*, No. 223. All the T atoms are tetrahedrally bonded to each other, forming an open framework of T_{46}. In the ideal structure, there are three crystallographically inequivalent site of 6c, 16i, and 24k in the Wyckoff notation. The two nonframework site, 2a and 6d, are the center of T_{20} and T_{24} polyhedra, respectively, and guest metal atoms occupy those sites. Full occupation of the nonframework sites by guest atoms, M, will give birth to the clathrate compound, M_8T_{46}.

In the present work, electronic structure calculations have been done for Si_{46} and $M_8Si_{38}Ga_8$ (M: Na, K, Rb, and Cs). Here, Ga is substituted into the framework Si, so as to fit the number of valence electrons to make the compound semiconducting. We also conducted calculations of di-Si, K_8Si_{46}, $Si_{38}A_8$, and $K_8Si_{38}A_8$ (A: Al, Ga, In) for comparison.

In order to determine the crystallographic parameters (lattice constants and fractional coordinates of atoms), geometrical optimization using total energy minimization algorithm has been performed. The site of substitution into Si framework by A atoms is not ordered but is described only by the occupancy probability. Since random positioning of the substituted site cannot be modeled by normal band calculation, we are obliged to select some specific atomic sites to be substituted. In addition, since some of the compounds considered here have not been obtained experimentally, we used the observed occupancy probability of crystallographical sites of $K_8Si_{38}Ga_8$ and $Rb_8Si_{38}Ga_8$ [8,9] so as to determine the sites of substitution of $M_8Si_{38}A_8$ by A. That is, 50% of Si 6c sites (three atoms) and 20% of Si 24k sites (five atoms) were assumed to be substituted by Ga (or, Al, In).

Table 1 presents the 54 assumed initial atomic positions of $M_8Si_{38}A_8$ in the *Pm*-3*m* structure using the Wyckoff notation. Atom numbers 1–6 are the 6c sites for the first group of Si, 7–22 are the 16i sites for the second group of Si, and 23–46 are the 24k sites for the third group of Si. 47–54 are the 2a and 6d sites for alkali metals. Si atoms in the three sites out of the 6c sites and those in the five sites out of the 24k sites are rather arbitrarily selected and assumed to be substituted by Ga (Al, In) in the model clathrate.

We performed geometrical optimization of these model clathrates and determined their lattice constants and the fractional coordinates of each atom. Introduction of this assumption means that the effect of random distribution of atoms was disregarded.

2.2. Details of calculations

The method of calculations is nearly the same as that used in our previous study[10] on the electronic structures of alkali metal monosilicides. That is, the calculations have been done using CASTEP (Cambridge Serial Total Energy Package) code developed by Payne et al. [11], which is a first-principle pseudopotential method based on the density-functional theory (DFT) in describing the electron–electron interaction, a pseudopotential description of the electron–core interaction, and a plane-wave expansion of the wavefunctions. The pseudopotential used is the ultrasoft pseudopotential generated by the scheme of Vanderbilt [12] which is bundled in the [2]Cerius[2] graphical User Interface. As for the method of approximation to the exchange-correlation term of the DFT, local density approximation (LDA) with generalized gradient correction[13] (Generalized-Gradient-corrected local density Approximation; GGA) was used.

'Total' one-electron band-structure energy can be obtained by integration of the density of the states (DOS), multiplied by band energy, with the energy from the bottom of the bands to the Fermi level. The Monkhorst–Pack scheme [14] with the spacing of 0.5 nm^{-1} in the reciprocal space was used for the *k*-points sampling for the total energy calculations. The kinetic cutoff energy of the plane wave expansion of the wavefunctions was set at 280 eV.

Crystallographic parameters of compounds are determined by the total energy minimization algorithm using the Broyden–Fletcher–Goldfarb–Shannon optimization procedure. We did not use full optimization process since this required too much computational time to obtain converged structure. Constraint conditions of the space group, however, seems not appropriate for the present study since not all the crystallographically equivalent sites are occupied by the same kind of atoms because of partial substitution of clathrate framework. Therefore, we only imposed the constraint condition of interaxial angle of the unit cell (=90°). The optimization process reached to different converged values of *a*, *b*, and *c* (=the lengths of the unit cell). Since the difference among them is not essential, we describe only the cell volumes to express converged structures, hereafter.

Convergence of an optimization mode is controlled by the following criteria: the energy change between two steps, the root-mean-square (rms) residual force on movable atoms, the rms displacement of atoms during the geometrical optimization process, and the rms residual bulk stress must be smaller than 1 meV, 10^{-10} N, 10^{-4} nm, and ±0.3 GPa, respectively.

The band structure (BS) calculations have been performed for optimized structures near their Fermi levels (E_F) along several high-symmetry lines in the Brillouin zone. The energy zero of the BS diagrams given below is taken at the top of the valence bands or the Fermi level.

Table 1
The initial atomic positions of the 54 atoms in the primitive cell of clathrates, based on the Adams et al.'s optimized data. Substitutional sites by the 13th group elements are based on Kröner et al.'s data, which is originally described using occupation probability. We assumed that eight sites (three sites out of 6c sites and five sites out of 24k sites) were substituted by Ga (or Al, In), which is described as 'A'. We also assumed that eight sites (2a and 6d) are fully occupied by guest alkali atoms, M.

Atom no.	Fractional coordinates			Atom
	x	*y*	*z*	
1	0	0.25	0.50	Si
2	0	0.75	0.50	A
3	0.50	0	0.25	Si
4	0.50	0	0.75	A
5	0.25	0.50	0	A
6	0.75	0.50	0	Si
7	0.1837	0.1837	0.1837	Si
8	−0.1837	−0.1837	0.1837	Si
9	−0.1837	0.1837	−0.1837	Si
10	0.1837	−0.1837	−0.1837	Si
11	0.6837	0.6837	0.3163	Si
12	0.3163	0.3163	0.3163	Si
13	0.6837	0.3163	0.6837	Si
14	0.3163	0.6837	0.6837	Si
15	−0.1837	−0.1837	−0.1837	Si
16	0.1837	0.1837	−0.1837	Si
17	0.1837	−0.1837	0.1837	Si
18	−0.1837	0.1837	0.1837	Si
19	0.3163	0.3163	0.6837	Si
20	0.6837	0.6837	0.6837	Si
21	0.3163	0.6837	0.3163	Si
22	0.6837	0.3163	0.3163	Si
23	0	0.1172	0.3077	A
24	0	−0.1172	0.3077	Si
25	0	0.1172	−0.3077	Si
26	0	−0.1172	−0.3077	Si
27	0.3077	0	0.1172	Si
28	0.3077	0	−0.1172	Si
29	−0.3077	0	0.1172	A
30	−0.3077	0	−0.1172	Si
31	0.1172	0.3077	0	Si
32	−0.1172	0.3077	0	Si
33	0.1172	−0.3077	0	Si
34	−0.1172	−0.3077	0	A
35	0.6172	0.5	0.1923	Si
36	0.3828	0.5	0.1923	Si
37	0.6172	0.5	0.8077	A
38	0.3828	0.5	0.8077	Si
39	0.5	0.8077	0.3828	Si
40	0.5	0.8077	0.6172	Si
41	0.5	0.1923	0.3828	A
42	0.5	0.1923	0.6172	Si
43	0.8077	0.6172	0.5	Si
44	0.8077	0.3828	0.5	Si
45	0.1923	0.6172	0.5	Si
46	0.1923	0.3828	0.5	Si
47	0	0	0	M
48	0.5	0.25	0	M
49	0.5	0.75	0	M
50	0.25	0	0.5	M
51	0.75	0	0.5	M
52	0	0.5	0.25	M
53	0	0.5	0.75	M
54	0.5	0.5	0.5	M

3. Results and discussion

At first, we calculated the electronic energy and the BS of Si_{46} and di-Si so as to compare the present results with those of previous

[2] Cerius[2] is a trademark of Accelrys Inc.

Table 2
Optimized lattice constants, cell volumes, and energies (E) of Si with the diamond structure and Si_{46} Type-I clathrate. Enthalpies (H) are also listed using $H = E + PV$ (P: hydrostatic pressure, V: cell-volume, where unit conversion is 1 GPa·nm^3 = 6.2415 eV). Their calculated band gaps are also listed.

Compound (external pressure)	Optimized lattice constant (nm^3)	volume/cell (nm^3)	volume/Si_1 (nm^3)	Calculated total energy (eV)	Calculated total enthalpy (eV)	Enthalpy/Si_1 (eV)	Calculated energy gap (eV)
Diamond/Si_2 (0 GPa)	0.3804	0.03894	0.01947	−217.4642	−217.4642	−108.7321	0.650
Diamond/Si_2 (+5 GPa)	0.3745	0.03715	0.01858	−217.4368	−216.2772	−108.1386	0.569
Diamond/Si_2 (−5 GPa)	0.3883	0.04139	0.02069	−217.4252	−218.7170	−109.3585	0.745
Clathrate/Si_{46} (0 GPa)	1.0033	1.0098	0.02195	−4998.3184	−4998.3184	−108.6591	1.315
Clathrate/Si_{46} (+5 GPa)	0.9889	0.9670	0.02102	−4997.6207	−4967.4403	−107.9878	1.213
Clathrate/Si_{46} (+10 GPa)	0.9735	0.9225	0.02005	−4995.6123	−4938.0272	−107.3484	1.065
Clathrate/Si_{46} (−5 GPa)	1.0294	1.0907	0.02371	−4997.3287	−5031.3699	−109.3776	1.537

calculations. Second, the BS of K_8Si_{46} was calculated. The density of states (DOS) of K_8Si_{46} has been already calculated by Moewes et al. [15] but we performed the calculation so as to compare the results with BS of Si_{46}. Third, we tried to clarify the effect of the substituted 13th group atoms into the Si_{46} framework on the BS of guest-free clathrates. In the end, we calculated the BSs of $M_8Si_{38}A_8$, especially for A = Ga. We also calculated the BS of $K_8Si_{38}Al_8$ and $K_8Si_{38}In_8$.

The results of calculations are summarized in Table 2 and Table 3, the details of which will be discussed below.

3.1. Elemental Si clathrate, Si_{46}, in comparison with Si with diamond structure

First, the results of optimization for di-Si and Si_{46} clathrate are described. The optimized lattice constants, cell volumes, and energies of di-Si and Si_{46} are shown in the 2nd, 3rd, and 5th columns of Table 2, respectively. Here, the calculations have been performed not only for the ambient pressure but also for assumed hydrostatic external pressures of −5 to +10 GPa. Those are performed for discussions later.

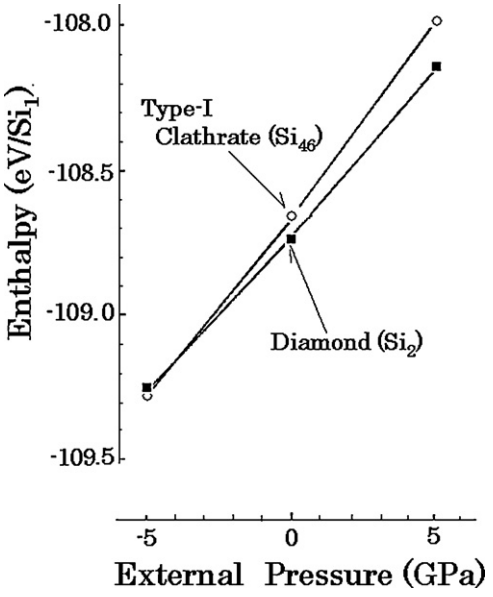

Fig. 1. The variation of the enthalpies per atom of Si with the diamond structure and the Si_{46} clathrate with the external pressures of −5 GPa to 5 GPa.

The observed lattice constant[3] for di-Si under the ambient pressure is 0.3840 nm. Therefore, the optimized lattice constant at 0 GPa (0.3804 nm) suggest a slight underestimation, as is often experienced in DFT-LDA (or GGA) calculations.

Predicted lattice constant of Si_{46} at ambient pressure (1.0033 nm) is 3% smaller than Adams et al.'s prediction (1.0355 nm). This is perhaps because their calculation is based on tight-binding method, which has a tendency to underestimate the overlap of bonding electrons.

The 6th column of Table 2 lists the enthalpy, $H = E + PV$, where E is the electronic energy calculated, P is the assumed hydrostatic pressure, and V is the optimized cell-volume.[4] The variation of the enthalpies per atom of di-Si and Si_{46} with the external pressures of −5 GPa to 5 GPa are presented in Fig. 1. From this figure, we can predict the relative stability of di-Si and Si_{46} at 0 K. At ambient pres-

Table 3
Optimized lattice constants, cell volumes, and calculated energy gaps of (a) Si_{46}, (b) K_8Si_{46}, (c) $Si_{38}A_8$ (A = Al, Ga, and In), (d) $M_8Si_{38}Ga_8$ (M = Na, K, Rb, and Cs), and (e) $K_8Si_{38}A_8$ (A = Al, Ga, and In). Gaps with asterisks mean compounds are not semiconducting; that is, their Fermi levels are not located in the gaps.

	Compounds	Optimized lattice constants (nm)	Volume/cell (nm^3)	Calculated energy gap (eV)
(a)	Si_{46}	$a = b = c = 1.0033$	1.0098	1.315
(b)	K_8Si_{46}	$a = b = c = 1.0216$	1.0661	1.227*
(c)	$Si_{38}Al_8$	$a = 1.0249$ $b = 1.0259$ $c = 1.0268$	1.0796	1.154*
	$Si_{38}Ga_8$	$a = 1.0263$ $b = 1.0266$ $c = 1.0266$	1.0816	1.114*
	$Si_{38}In_8$	$a = 1.0516$ $b = 1.0535$ $c = 1.0566$	1.1705	0.946*
(d)	$Na_8Si_{38}Ga_8$	$a = 1.0301$ $b = 1.0278$ $c = 1.0321$	1.0928	0.448
	$K_8Si_{38}Ga_8$	$a = 1.0407$ $b = 1.0403$ $c = 1.0418$	1.1280	0.798
	$Rb_8Si_{38}Ga_8$	$a = 1.0423$ $b = 1.0421$ $c = 1.0435$	1.1334	0.824
	$Cs_8Si_{38}Ga_8$	$a = 1.0529$ $b = 1.0528$ $c = 1.0539$	1.1681	0.891
(e)	$K_8Si_{38}Al_8$	$a = 1.0371$ $b = 1.0365$ $c = 1.0372$	1.1150	0.791
	$K_8Si_{38}Ga_8$	$a = 1.0407$ $b = 1.0403$ $c = 1.0418$	1.1280	0.789
	$K_8Si_{38}In_8$	$a = 1.0700$ $b = 1.0702$ $c = 1.0729$	1.2286	0.715

[3] It should be noted that the lattice constants for di-Si is not for the conventional unit cell (Si_8); rather, they correspond to the reduced primitive cells of Si_2.

[4] For example, enthalpy of Si_2 at 5 GPa is the sum of its energy, −217.4368 eV, and PV, 0.1858 GPa·nm^3 or 1.1596 eV, where conversion of 1 GPa·nm^3 = 6.2415 eV is used.

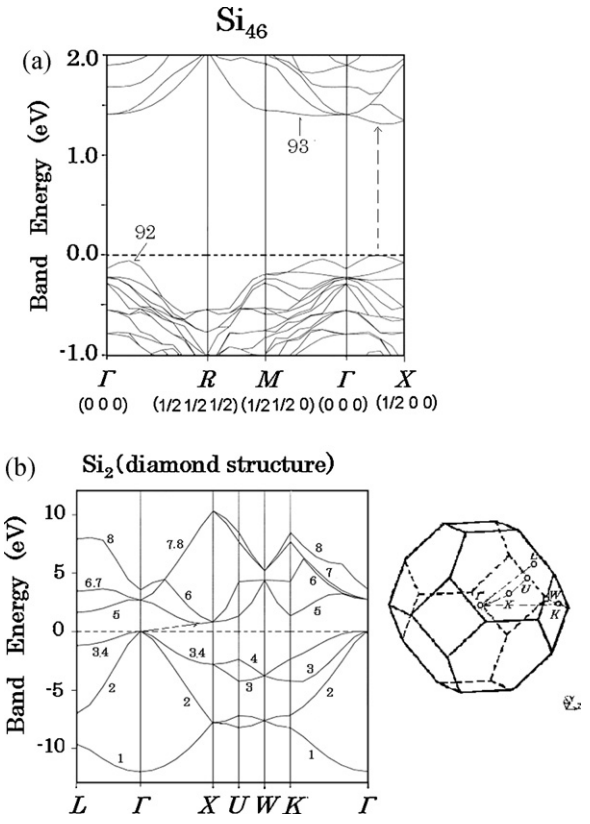

Fig. 2. (a) Band structure of the Si_{46} clathrate. The energy zero in this and succeeding band diagrams of semiconducting compounds ((b) and Fig. 5) are taken at the top of valence bands. Dashed arrow in this and succeeding band diagrams show a line connecting the top of the valence bands and the bottom of the conduction bands. (b) Band structure of Si with the diamond structure. Inset shows the Brillouin zone.

sure and higher pressure, di-Si is stable, whereas Si_{46} is stable at negative pressure below *ca.* −4GPa. This is similar to the result of previous calculation [16] for Type-II Si clathrate, Si_{136}, based on the energy *vs.* volume relations of Si_{136} and di-Si.

The BS of Si_{46} at the ambient pressure is shown in Fig. 2(a). Also shown for comparison in Fig. 2(b) is that of di-Si. As is well-known, di-Si is an indirect semiconductor. The valence band maximum (VBM) is at Γ (0 0 0) and the conduction band minimum (CBM) is along the line from Γ to X (1/2 0 1/2), which is in accordance with the previous calculation [17].

The band gap (E_g) calculated here was 0.65 eV, which is about 0.5 eV narrower than the observed value (1.17 eV). This is a well-known discrepancy of the DFT calculation using LDA and GGA. However, it is also known that one can expect the GGA to predict trends of E_g value correctly. So, a comparison of this E_g value with that of the clathrate phase is likely to be meaningful.

In contrast to di-Si, Fig. 2(a) shows that Si_{46} is a direct semiconductor. Both of VBM and CBM are along the line from Γ (0 0 0) to X (1/2 0 0) and the calculated direct gap value between the 92nd and 93rd band is 1.315 eV. This value is *ca.* 0.7 eV wider than that of di-Si. Thus, *ca.* 0.7 eV opening of the Si band gap was reproduced, though absolute gap values are different from those of previous calculations [2,18].[5]

[5] E_g of Si in diamond structure calculated by Adams et al. is 1.7 eV, while that of Si_{46} is 2.5 eV [2].

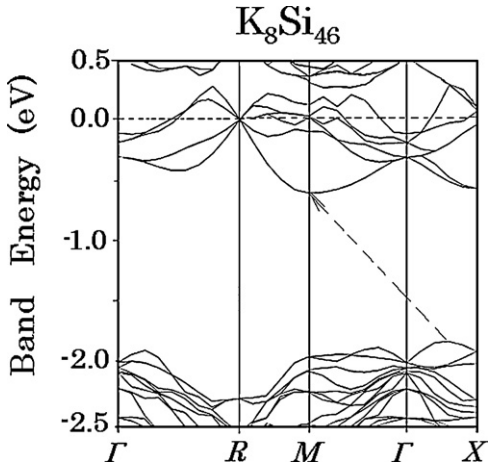

Fig. 3. Band structure of K_8Si_{46}. The energy zero is taken at its Fermi level.

3.2. Binary Si clathrate with potassium guests

As is shown in the previous section, guest-free Si_{46} is unstable compared to di-Si in the ambient (and under higher pressures). However, alkali-metal incorporation makes this Type-I clathrate structure stable. For example, K_8Si_{46}, which has fully occupied framework of Type-I silicon clathrate, was synthesized [19].

The result of optimization calculation of K_8Si_{46} is given in (b) of Table 3, along with other clathrate compounds which will be discussed later. The optimized lattice constant, 1.0216 nm, shows again slight underestimation(∼0.6%) compared to the observed one (=1.0275 nm [20]).

The density of states (DOS) of K_8Si_{46} has been calculated by Moewes et al. [15] using 384 *k*-points in the first Brillouin zone. The main features on total and partial DOS are reported to be very similar with guest-free Si_{46}. Differences occur mainly in the degree of filling of the energy bands by valence electrons and the energy position with respect to the Fermi level. They concluded that the form of DOS curve does not show strong modification upon the inclusion of K atoms, which is due to weak hybridization between Si_{46} and K states, indicating that, (1) metal–metal and metal–silicon interaction are ionic and (2) K act as electron donors.

In the present study, we calculated BS of K_8Si_{46}. The result is shown in Fig. 3. A shape of the band structure is nearly the same as that of Si_{46} but the band energy at M is remarkably lowered and the bottom of the conduction bands below the Fermi level (E_F) is located at M. This result is a bit different from that of Na_8Si_{46} [21], where bottom of conduction bands is located at X.

E_F shifts to higher energy side as expected from simple filling of empty conduction band of Si_{46} with eight electrons. As a result, E_F moves into the conduction band of Si_{46}, which indicates that K_8Si_{46} is a metal. Energy gap still exists 0.68 eV below E_F. The value of E_g is 1.227 eV, becoming narrower than that of Si_{46} (=1.315 eV) but 0.58 eV larger than that of di-Si (=0.65 eV).

3.3. Introduction of the 13th group element into the Si clathrate framework

As stated above, removal of eight valence electrons from K_8Si_{46} by substitution of eight 13th group atoms for eight Si atoms results in formation of a semiconducting Si clathrate. Therefore, we tried to clarify the effect of the 13th group atoms on E_g. Before calculating BS of, *for example*, $K_8Si_{38}Ga_8$, we investigated the effect of substitutional 13th group element into the Si_{46} framework. The results

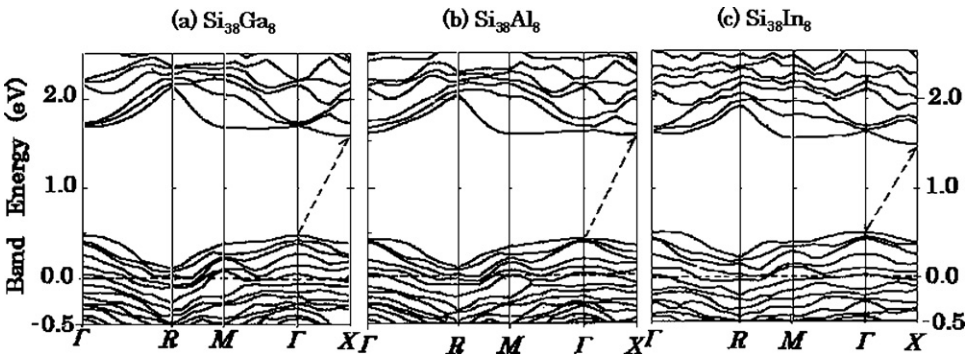

Fig. 4. Band structures of $Si_{38}Ga_8$, $Si_{38}Al_8$, and $Si_{38}In_8$. The energy zero is taken at its Fermi level.

of optimization for $Si_{38}A_8$ (A = Al, Ga, and In) are shown in (c) of Table 3. Their optimized cell volumes are *ca.* 1.08 nm^3, 1.08 nm^3 and 1.17 nm^3, which are larger than that of Si_{46} (=1.01 nm^3). This tendency can be expected from the covalent radii for single bonds by Pauling; Si (=0.117 nm), Al (=0.125 nm), Ga (=0.125 nm) and In (=0.150 nm).

Fig. 4 shows the calculated BS of $Si_{38}A_8$ (A = Ga, Al, and In).

Though shapes of the BSs are alike to each other, they are somewhat different from expectation of simple removal of valence electrons from Si_{46}. That is, the top of the valence band moves to Γ, while the bottom of the conduction band moves to X. This suggests the hybridization between Si and A. The Fermi level (E_F) shifts to lower energy side and is located in the valence band, as expected. Energy gaps (E_g) exist *ca.* 0.4 eV above E_F. The values of E_g are 1.11 eV for $Si_{38}Ga_8$, 1.15 eV for $Si_{38}Al_8$, and 0.95 eV for $Si_{38}In_8$ and they are all narrower than Si_{46} though still larger than that of di-Si. The effect of the substitutional elements of Si framework is not so remarkable, especially in the cases of Al and Ga.

3.4. Ternary Si clathrate compounds, $M_8Si_{38}A_8$ (M = Na, K, Rb, Cs; A = Ga, Al, In)

Since the synthesized Si clathrates at present are rather limited to those based on Si–Ga framework, most of our calculations here have been performed for $M_8Si_{38}Ga_8$ (M = Na, K, Rb, and Cs). The results of optimization are shown in (d) of Table 3.

The optimized cell volumes of $K_8Si_{38}Ga_8$ and $Rb_8Si_{38}Ga_8$ are 1.128 nm^3 and 1.133 nm^3, respectively, which are 99.4% and 98.8% of observed values(1.134 nm^3 and 1.147 nm^3). These values correspond to 0.2% and 0.4% underestimation of the lattice constants.

The calculated BSs of $M_8Si_{38}Ga_8$ are shown in Fig. 5. Eight alkali metal atoms in the nonframework sites and eight Ga atoms in the framework sites compensate each other and make $M_8Si_{38}Ga_8$ a semiconductor.

Their tops of the valence band are located at Γ, just the same as in the case of $Si_{38}Ga_8$, while the bottoms of the conduction band move to X in case of $Na_8Si_{38}Ga_8$, or to M in case of $K_8Si_{38}Ga_8$, $Rb_8Si_{38}Ga_8$ and $Cs_8Si_{38}Ga_8$. This movement in case of $K_8Si_{38}Ga_8$ and $Na_8Si_{38}Ga_8$ is similar to the change seen in the BS from Si_{46} to K_8Si_{46} and Na_8Si_{46}, above stated.

Thus, they are all indirect semiconductors with the calculated gaps of 0.448 eV ($Na_8Si_{38}Ga_8$), 0.798 eV ($K_8Si_{38}Ga_8$), 0.824 eV ($Rb_8Si_{38}Ga_8$), and 0.891 eV ($Cs_8Si_{38}Ga_8$). The gaps become wider with the promotion to the heavier encapsulated guest alkali atoms.

We consider that one of the possible reasons for this behavior is a cell-volume effect of Si clathrate. It is known that di-Si will have negative coefficient of the pressure dependence of E_g [22]. A similar effect would work in case of the Si_{46} clathrates. The calculated E_g's of $M_8Si_{38}Ga_8$ are plotted in Fig. 6 as a function of the cell-volumes, accompanied by the calculated cell-volume dependence of E_g's of

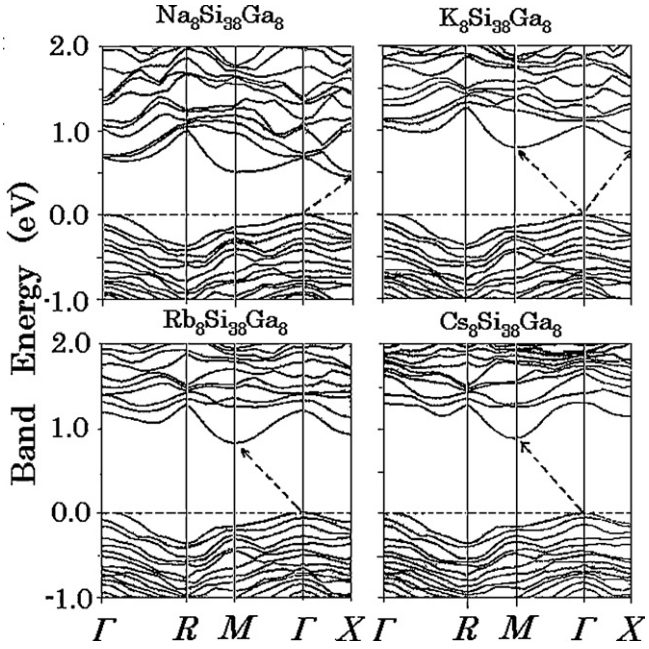

Fig. 5. Band structures of $Na_8Si_{38}Ga_8$, $K_8Si_{38}Ga_8$, $Rb_8Si_{38}Ga_8$, and $Cs_8Si_{38}Ga_8$.

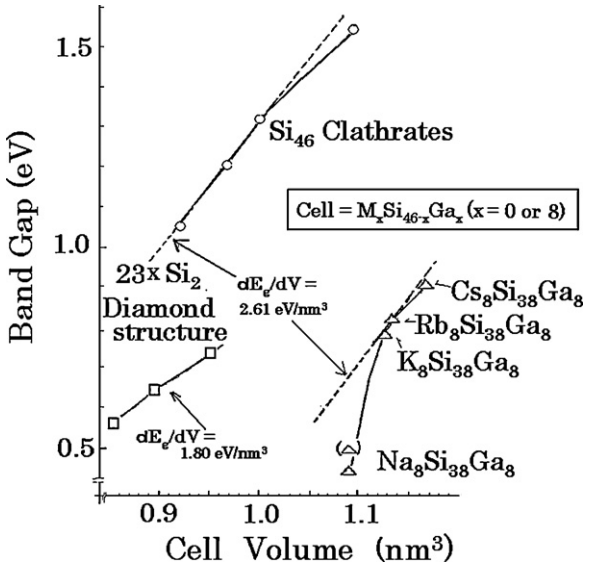

Fig. 6. Calculated band gaps of $M_8Si_{38}Ga_8$ (M: Na, K, Rb, and Cs) as a function of their cell-volumes. Those of Si_{46} clathrate and Si with diamond-like structure are also shown. A dashed line indicates the plot of $dE_g/dV = 2.61$ eV/nm^3. The gap value shown by an open triangle in parentheses is the energy difference between the top of Γ and bottom of M of $Na_8Si_{38}Ga_8$.

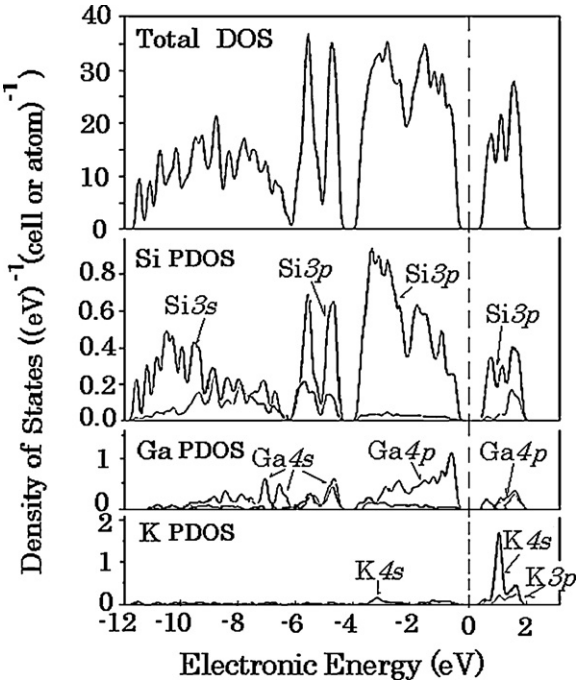

Fig. 7. Total and partial densities of states of $K_8Si_{38}Ga_8$.The energy zero is taken at its Fermi level.

Si_{46} and di-Si,[6] which has already been shown in the 8th column of Table 2. E_g of Si_{46} has positive coefficient of the cell volume dependence of 2.61 eV/nm^3. This tangent was also plotted by a dashed line in the figure for ease of understanding. A rough tendency of E_g of $M_8Si_{38}Ga_8$ can be explained by this cell-volume effect. However, a deviation of E_g of $Na_{38}Si_{38}Ga_8$ from this dashed line is also found. We consider two possible reasons for that.

One is the difference in the positions of VBM and CBM. In $Cs_8Si_{38}Ga_8$, $Rb_8Si_{38}Ga_8$, and $K_8Si_{38}Ga_8$, VBMs are located at Γ while CBMs are at M. In $Na_8Si_{38}Ga_8$, VBM is also located at Γ while CBM is at X. The energy difference between VBM at X and CBM at M is 0.506 eV, about 60 meV wider than E_g of $Na_{38}Si_{38}Ga_8$. This value is plotted in Fig. 6 by an open triangular in parentheses. It should be also noted that the E_g's for Si_{46} plotted in Fig. 6 are the energy difference of VBM and CBM at the center of Γ and X. If we use the energy differences between VBM at Γ and CBM at X, the values are 1.732 eV for cell volume of 1.0907 nm^3, 1.485 eV for 1.0033 nm^3, 1.387 eV for 0.987 nm^3 and 1.201 eV for 0.9225 nm^3. Though not plotted in the figure, dE_g/dV value is 3.3 eV/nm^3, a bit larger than 2.61 eV/nm^3 above stated. Both of these two factors considered here decrease the apparent deviation of E_g of $Na_{38}Si_{38}Ga_8$ from the dashed line.

Another possible reason for the deviation of E_g of $Na_{38}Si_{38}Ga_8$ from the dashed line is difference in electropositivity of alkali-metals.

We present the partial densities of states of $K_8Si_{38}Ga_8$ in Fig. 7. Valence bands (VB) of $K_8Si_{38}Ga_8$ are mainly composed of atomic orbitals (AOs) of Si and Ga while contribution of AOs of alkali metals to conduction bands (CB) is great, though AO of Si also contribute to some extent. We have already shown the tendency that E_g values of alkali-metal monosilicides are increased as their ionicities are increased [10]. The similar effect would work in the present case. That is, more electropositive elements will raise the energy level of CB, resulting in wider E_g. Since Na is less electropositive than other alkali-metals, this effect will not work so much, resulting in narrower E_g-values than expected from the cell-volume effect.

As for the effect of the 13th group elements in the clathrate framework, we give the results for $K_8Si_{38}Al_8$ and $K_8Si_{38}In_8$ in (e) of Table 3. They are both indirect semiconductors with the E_g values of 0.791 eV and 0.715 eV, respectively. Compared to the value of 0.789 eV for $K_8Si_{38}Ga_8$, it can be said that the effect of 13th group elements is not so large, though the clathrate including In as framework would have narrower E_g than corresponding clathrates including Al or Ga. The same would be expected for other $M_8Si_{38}A_8$.

In the end of the present study, we would like to mention about the possible deviations of the present results under the constraint condition of $\alpha = \beta = \gamma = 90^\circ$, from the results of fully optimized structures. The convergence process under the full optimization conditions, where so many parameters are simultaneously varied, was sometime poorly stable. Since introduction of the above constraint condition improved the convergence process, we adopted them as stated in Section 2. However, one may doubt whether there might be much difference among the converged structures using different constraint conditions. Therefore, in order to evaluate the possible effect of the constraint conditions, we restarted a full-optimization of the optimized structures under the above constraint condition. The results for $K_8Si_{38}Ga_8$ are as follows: (A) the converged structure under the above constraint conditions is a = 1.0407 nm, b = 1.0403 nm, c = 1.0418 nm, $\alpha = \beta = \gamma = 90^\circ$, and the cell volume = 1.1280 nm^3. (B) The converged structure under full optimization is a = 1.0406 nm, b = 1.0401 nm, c = 1.0417 nm, $\alpha = 89.85^\circ$, $\beta = 89.99^\circ$, $\gamma = 89.90^\circ$, and the cell volume = 1.1275 nm^3. Thus, the unit cell volume could be made smaller by relaxing the interaxial angles, and the electronic energy for (B) was more negative than (A) by 0.133 eV. This error is, however, small enough, we think. We also would be able to expect the same for other compounds and the results described here would be proper for full-optimized structures.

4. Conclusion

Band structure calculations have been performed for fully occupied, ordered model of Type-I clathrates, $M_8Si_{38}A_8$ (M = Na, K, Rb, and Cs; A = Ga, Al, and In) using the density-functional theory with the generalized gradient corrected local density approximation. It was found that they are indirect semiconductors. The calculated gaps of $Na_8Si_{38}Ga_8$, $K_8Si_{38}Ga_8$, $Rb_8Si_{38}Ga_8$, and $Cs_8Si_{38}Ga_8$ are 0.448 eV, 0.798 eV, 0.824 eV, and 0.890 eV, respectively. These are wider or narrower than the calculated gap of 0.65 eV for Si with diamond structure. The tendency of gap widening with the promotion to the heavier encapsulated guest alkali atoms are discussed with the viewpoint of cell-volume dependence of band gap of Si_{46} and the electropositivity of guest alkali atoms encapsulated. The effect of A, 13th group elements, is not so remarkable. Since calculations are based on the idealized model, there may be discrepancy between calculated values and observed values due to the random positioning of the atoms, vacancies, nonstoichiometry, and so on. However, we hope that our predictions will prove useful in better understanding of semiconducting Si clathrates.

Acknowledgment

This research was partially supported by Scientific Research on Priority Areas of New Materials Science Using Regular Nano Spaces, the Ministry of Education, Culture, Sports, Science and Technology, Grant-in-Aid for 22013019.

[6] The calculations for di-Si were performed in order to confirm the validity of the present calculation. The calculated E_g dependence on cell-volumes of 23 × Si_2 was +1.80 eV/nm3 and the cell-volume dependence on pressure is −0.00975 nm^3/GPa. The product of these gives −0.0175 eV/GPa, which is close to the observed value of −15 meV/GPa [22]. This would guarantee the validity of the present calculations.

References

[1] J.S. Kasper, P. Hagenmuller, M. Pouchard, C. Cros, Science 150 (1968) 1713.
[2] G.B. Adams, M.A. O'Keeffe, A. Demkov, O.F. Sankey, Y.M. Huang, Phys. Rev. B 49 (1994) 8048.
[3] D. Connétable, V. Timoshevskii, E. Artacho, X. Blase, Phys. Rev. Lett. 87 (2001) 206405.
[4] H. Kawaji, H. Horie, S. Yamanaka, M. Ishikawa, Phys. Rev. Lett. 74 (1995) 1427.
[5] G.S. Nolas, J.L. Cohen, G.A. Slack, S.B. Schujman, Appl. Phys. Lett. 73 (1998) 178.
[6] M. Imai, A. Sato, H. Udono, Y. Imai, H. Tajima, submitted for publication.
[7] M. Christensen, S. Johnsen, B.B. Iversen, Dalton Trans. 39 (2010) 978.
[8] R. Kröner, K. Peters, H.G. Schnering, R. Nesper, Z. Kristallorgr, NCS 213 (1998) 667.
[9] H.G. Schnering, R. Kröner, H. Menke, K. Peters, R. Nesper, Z. Kristallorgr, NCS 213 (1998) 677.
[10] Y. Imai, A. Watanabe, J. Alloys Compd. 478 (2009) 754.
[11] M.C. Payne, M.P. Teter, D.C. Allan, T.A. Arias, J.D. Joannopoulos, Rev. Modern Phys. 64 (1992) 1045.
[12] D. Vanderbilt, Phys. Rev. B 41 (1990) 7892.
[13] J.P. Perdew, Y. Wang, Phys. Rev. B 46 (1992) 6671.
[14] H.J. Monkhorst, J.D. Pack, Phys. Rev. B 13 (1976) 5188.
[15] A. Moewes, E.Z. Kurmaev, J.S. Tse, M. Geshi, M.J. Ferguson, V.A. Trofimova, Y.M. Yarmoshenko, Phys. Rev. B 65 (2002) 153106.
[16] J. Dong, O.F. Sankey, G. Kern, Phys. Rev. B 60 (1999) 950.
[17] J.R. Chelikowsky, M.L. Cohen, Phys Rev. B 14 (1976) 556.
[18] S. Saito, A. Oshiyama, Phys. Rev. B 51 (1995) 2628.
[19] See, for example G.K. Ramachandran, P.F. McMillan, J. Dong, O.F. Snakay, J. Solid State Chem. 154 (2000) 626, and references therein.
[20] J.S. Tse, S. Desgreniers, Z.Q. Li, M.R. Ferguson, Y. Kawazoe, Phys. Rev. Lett. 89 (2002) 195507.
[21] J.S. Tse, K. Uehara, R. Rousseau, A. Ker, C. Ratcliffe, N.A. White, G. MacKay, Phys. Rev. Lett. 85 (2000) 114.
[22] Y. Ishikawa, T. Kobayashi, A.D. Prins, J. Nakahara, M.A. Lourenco, R.M. Gwilliam, K.P. Homewood, Phys. Status Solidi 244 (2007) 402.